Journal of *Marine Science and Engineering*

MDPI

Article

Formation of MASS Collision Avoidance and Path following Based on Artificial Potential Field in Constrained Environment

Xiangyu Chen [1], Miao Gao [1,*], Zhen Kang [1], Jian Zhou [2], Shuai Chen [1], Zihao Liao [1], Haixin Sun [3] and Anmin Zhang [1,4,*]

[1] School of Marine Science and Technology, Tianjin University, Tianjin 300072, China
[2] Jiangsu Automation Research Institute, Lianyungang 222061, China
[3] School of Informatics, Xiamen University, Xiamen 361005, China
[4] Tianjin Port Environmental Monitoring Engineering Center, Tianjin 300072, China
* Correspondence: gaomiao@tju.edu.cn (M.G.); zhanganmin@sina.com (A.Z.)

Abstract: It is essential to promote the intelligence and autonomy of Maritime Autonomous Surface Ships (MASSs). This study proposed an automatic collision-avoidance method based on an improved Artificial Potential Field (APF) with the formation of MASSs (F-MASSs). Firstly, the navigation environment model was constructed by the S-57 Electronic Navigation Chart (ENC) data in Tianjin Port. The Formation Ship State Parameter (FSSP) definition was proposed for the port environment under multiple constraints that considered the navigation conditions of the MASSs. The formation pattern transformation was settled by changing the formation ship state parameter. Considering the constraints of an 'unmanned–manned' encounter situation, the static obstacles, and the design of the channel area improved artificial potential method for the formation. Finally, the simulation experiment was carried out in the sea near Tianjin Port to verify the effectiveness of the algorithm under multiple constraints. The results indicate that the method can satisfy the integrated operation of collision avoidance and path following in a constrained environment, and it can support the application of merchant F-MASS autonomous navigation in the future.

Keywords: maritime autonomous surface ship; collision avoidance; path following; artificial potential field; constrained environment

Citation: Chen, X.; Gao, M.; Kang, Z.; Zhou, J.; Chen, S.; Liao, Z.; Sun, H.; Zhang, A. Formation of MASS Collision Avoidance and Path following Based on Artificial Potential Field in Constrained Environment. *J. Mar. Sci. Eng.* **2022**, *10*, 1791. https://doi.org/10.3390/jmse10111791

Academic Editor: Gerasimos Theotokatos

Received: 31 October 2022
Accepted: 17 November 2022
Published: 21 November 2022

1. Introduction

Over the past few decades, the development of Maritime Autonomous Surface Ship (MASS) has been very rapid. MASS can carry out tasks including cargo transportation, search and rescue, coastal patrol, and security incessantly with less human intervention. Compared with common ships, MASS reduces the interference of human factors in terms of ship control, ship command execution, and human–computer interaction. MASS is gradually moving from the laboratory to real navigation environments.

The International Maritime Organization (IMO) held a Legislative Framework Development Workshop for MASS on 5–6 September 2022 [1], which covered a wide range of topics regarding MASS including MASS safe operation requirements, MASS technology status reports and deployment, future prospects for MASS research and development, and legal issues and obstacles to overcome to ensure that MASS operations comply with international legislation, including the United Nations Convention on the Law of the Sea (UNCLOS). Given that MASS may operate in a mixed-traffic environment that is highly dependent on the interaction among systems, it is necessary to ensure that MASS and common ships can operate safely together. Therefore, the study is very important to combine a swarm of MASS with common ships in a constrained environment.

In 2021, the European Maritime Safety Agency (EMSA) released its Annual Overview of Marine Casualties and Incidents 2021, in which a total of 15,481 marine casualties were reported from 2014 to 2020 [2]. The number of marine casualties reported each year has

increased from 2014 to 2019, with the number of marine casualties falling by 10.1% in 2020. The main cause of the casualties was loss of control of the ship (32.3%), followed by collision and contact casualties (30.2%); the data are shown in Figure 1. About 53.5% of the casualties investigated were caused by personnel misconduct. The nonconformities encountered in the use of technology by humans were counted [3]. Therefore, human error will be permanent in maritime transport. The intelligent navigation research of MASS can effectively deal with the impact on navigation safety caused by human factors or errors. MASS can replace some common or high-risk manual operations.

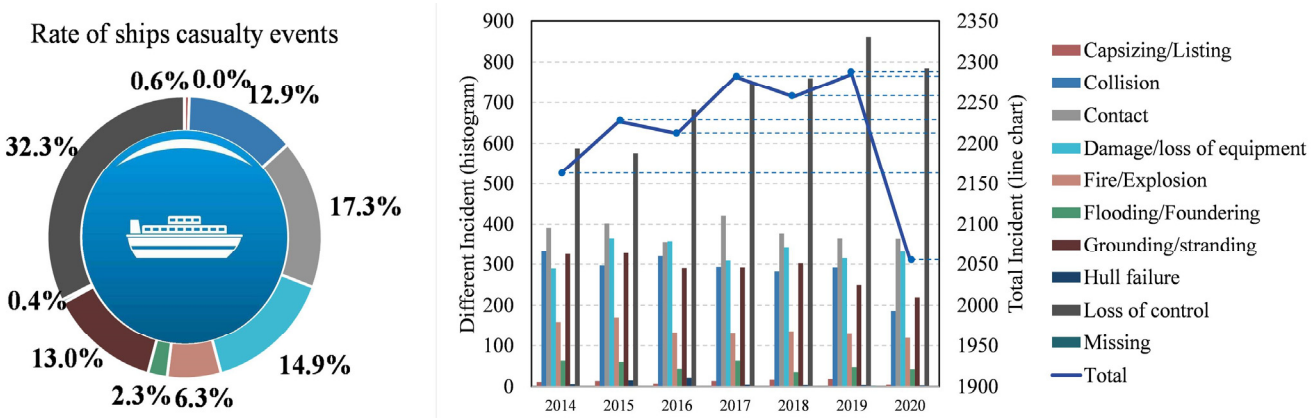

Figure 1. Distribution of casualty events with a ship.

Recently, the research on the swarm of MASS has become a hot spot in the field of ship navigation, and the development trend of ships is gradually moving toward the direction of unmanned/fewer people on ships, intelligence, and swarming [4]. Compared with a single vessel, the swarm of MASS has a wider range of application scenarios and business value. Multiple tasks can be completed at the same time in a complex environment by the swarm of MASS, which can economize a lot of human resources and avoid collisions on the sea, and MASS also can work continuously without considering the risks caused by human factors [5]. However, compared with a single vessel, a swarm of MASSs is faced with a more complex navigation environment when executing tasks [6]. A swarm of MASS needs to consider the position of other ships and maintain path following and collision avoidance during the autonomous navigation period.

Some scholars have carried out extensive studies on Unmanned Surface Vehicle (USV)/MASS path planning, single-ship collision avoidance, multiship collision avoidance, and many related optimization algorithms are being applied to MASS. In path planning, the A* algorithm can help the object to find a complete path, and the traditional A* algorithm is improved to achieve path planning in multiple constraints [7]. The Particle Swarm Optimization (PSO) algorithm realizes optimal path finding [8]. The improved Ant Colony Optimization (ACO) algorithm speeds up the node search speed [9]. The Fast Marching Method (FMM) can improve computational efficiency [10]. The improved genetic algorithm can avoid local optimization and realize parallel task allocation and path planning [11].The path planning algorithm mentioned above usually takes a single agent as the experimental object, and the simulation environment is far different from the real navigation environment. It cannot meet the path planning requirements for swarm of MASS, so maintaining the stability of the swarm structure is particularly important.

Another problem for the swarm of MASS is path following and collision avoidance [12]. The dynamic window method is used to avoid collisions in a dynamically unpredictable environment [13]. A fuzzy dynamic collision risk model for collision risk, navigation economy, and collision-avoidance time is considered [14]. The Real-time Collision-avoidance Algorithm is based on the Field Theory [15]. The Artificial Potential Field (APF) method is an effective method to satisfy the demands of collision avoidance and path following. The

APF method adjusts the potential energy gradient descent of the MASS in the process of path following by establishing the environmental potential field and maintaining the preset route of the MASS. Meanwhile, this method also can attain a reasonable circumambulation according to the influential range of the obstacle as an attempt to achieve the effect of collision avoidance. Therefore, the APF method was used to solve the problem of ship autonomous navigation.

Recently, many studies combined the APF method with other path optimization algorithms to solve the problem of autonomous navigation in a complex environment. A two-layer dynamic obstacle avoidance algorithm was proposed by combining the Velocity Obstacle (VO) method with the APF method [16]. A collision-avoidance path-planning method based on a hybrid APF method was proposed [17]. In a complex unknown environment, the APF method is used for the swarm of MASS collision avoidance [18].

In the process of sailing, the swarm of MASS needs to avoid external obstacles (land, islands, and target ships) and internal collision risks (swarm members). After selecting an appropriate strategy, the swarm can adjust the conditions of the member ships, which can transform into a regular formation. The formation is a stable condition in which multiple MASSs coexist. Distributed formation control for the trajectory of Underactuated Underwater Vehicles (UUVs) has achieved high effectiveness [19]. Kuppan integrated the distributed formation framework and dynamic role-switching mechanism [20]. Sun proposed an autonomous navigation system for USVs with the distributed control strategy [21]. The Distributed Leader–Follower strategy is used for fully actuated USVs to achieve a formation path following with constraints [22]. Trajectory tracking is achieved by applying deep reinforcement learning to the brake speed constraints with the formation of USVs [23]. However, in the changeable environment and engineering application, it is difficult for F-MASSs to complete the optimal path following under the interference of multiple uncertain factors. Therefore, the feasible goal is to find a navigable path-following scheme for F-MASSs.

It is a challenge for MASSs to coexist with common ships in a high interaction in channel systems. Tonoğlu et al. provided the estimation of potential risks in the Turkish Straits through a Fuzzy AHP-PRAT method [24]. Christensen et al. discussed the future potential of the northern sea route as a viable and less risky alternative way for shipping trade [25]. Xiao and Ma studied collision-avoidance measures and behaviors of autonomous ships in the channels based on AIS data, which was helpful to develop navigation traffic simulation scenarios to reflect ship behaviors in reality [26]. Wang studied the navigability of the restricted channel, reflecting the change of traffic efficiency caused by the behavior of ships in the restricted channel [27]. However, a F-MASS encounters other common ships in the channel, and the operation of MASSs and common ships is still controversial. Therefore, the study of MASS decision making in the restricted channel is helpful to solve the current problem.

The MASS can move clearly according to preset paths and commands, while the common ship (manned ship) cannot obtain the subsequent maneuvering information. Under the 'unmanned–manned' encounter situation, the avoidance decision made between the two ships has become a hot issue in current research. Previous scholars classified MASSs and manned ships as the same engine ship in the International Regulation for Preventing Collision at Sea (COLREGs) rules and considered that the MASS has the same avoidance priority as a manned ship when it encounters a common ship [28,29]. Under COLREGs rules, even if the MASS is the stand-on vessel, it will not act to the give-way vessel, and the stand-on vessel still needs to make emergency avoidance action for the give-way vessel [30]. Given the complex situation of multiship encounters at sea, a fuzzy inference system has been established to infer the sailing intention of other ships to assist in MASS collision avoidance [31]. The method of dynamic navigation ship domain was adopted to find navigable paths from both sides of the stand-on vessel [32]. Therefore, it is meaningful to deal with the 'unmanned–manned' encounter situation based on previous experience.

Previous work included extracting various modes of ship encounters using AIS data, constructing a division map of ship confluence azimuth to assist ships in path planning and intelligent collision avoidance [33], and studying the avoidance decision making of F-MASSs when encountering common ships. The relevant topographic coordinates of Tianjin Port were extracted from the S-57 Electronic Navigation Chart (ENC). The trajectory of the common ship was retrieved from AIS data.

Inspired by the abovementioned literature, this article aims at resolving the collision-avoidance and path-following problems of F-MASSs by employing the improved APF method in the constrained environment. Some highlights can be the following: (1) Based on the Leader–Follower strategy, a variable formation strategy is introduced to meet the constraint condition of formation. (2) To satisfy the multiple constraints of F-MASSs, a novel formation condition set was designed for the F-MASSs, and the different priority conditions were listed. (3) The traditional APF method was improved for the path-following process of F-MASSs. Finally, the simulation results validate the effectiveness of our improved APF method in 'unmanned–manned' encounter situations and constrained environments.

The organizational division of the paper is as follows: The first section is the introduction. The second section is about problem description, including the assumptions and the formation strategy. The third section is the methodology, including definition of Formation Ship State Parameter and the improved APF method. The fourth section introduces the environment model and the verification simulation experiment. Finally, this paper is summarized. The section structure is shown in Figure 2, and the full text structure diagram is shown in Figure 3.

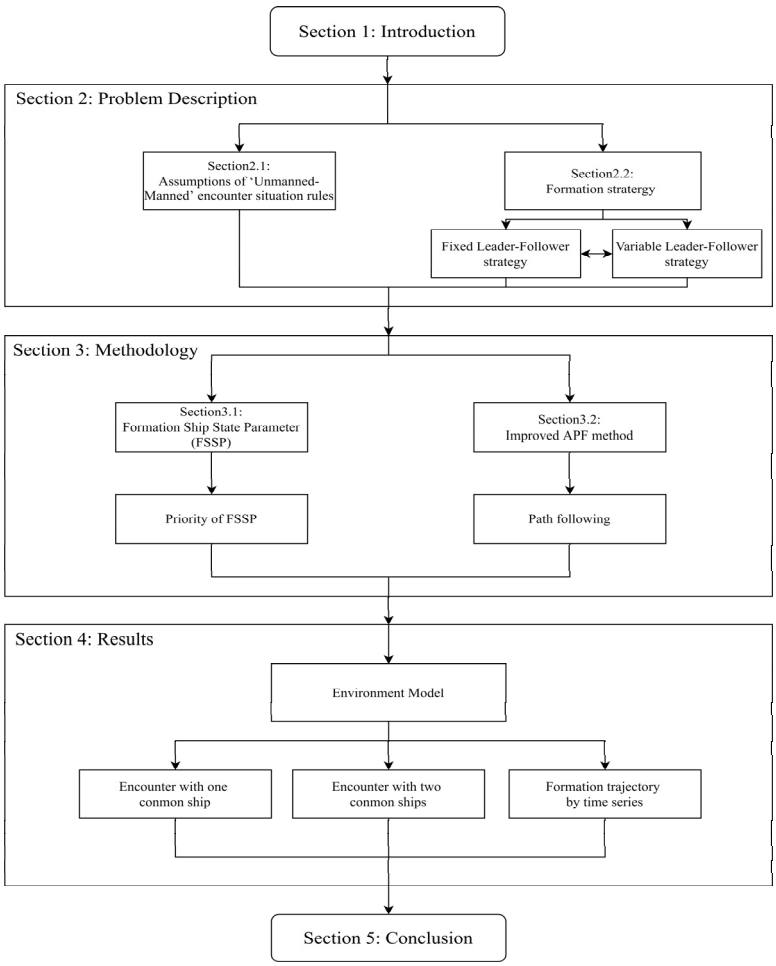

Figure 2. Section structure diagram of this paper.

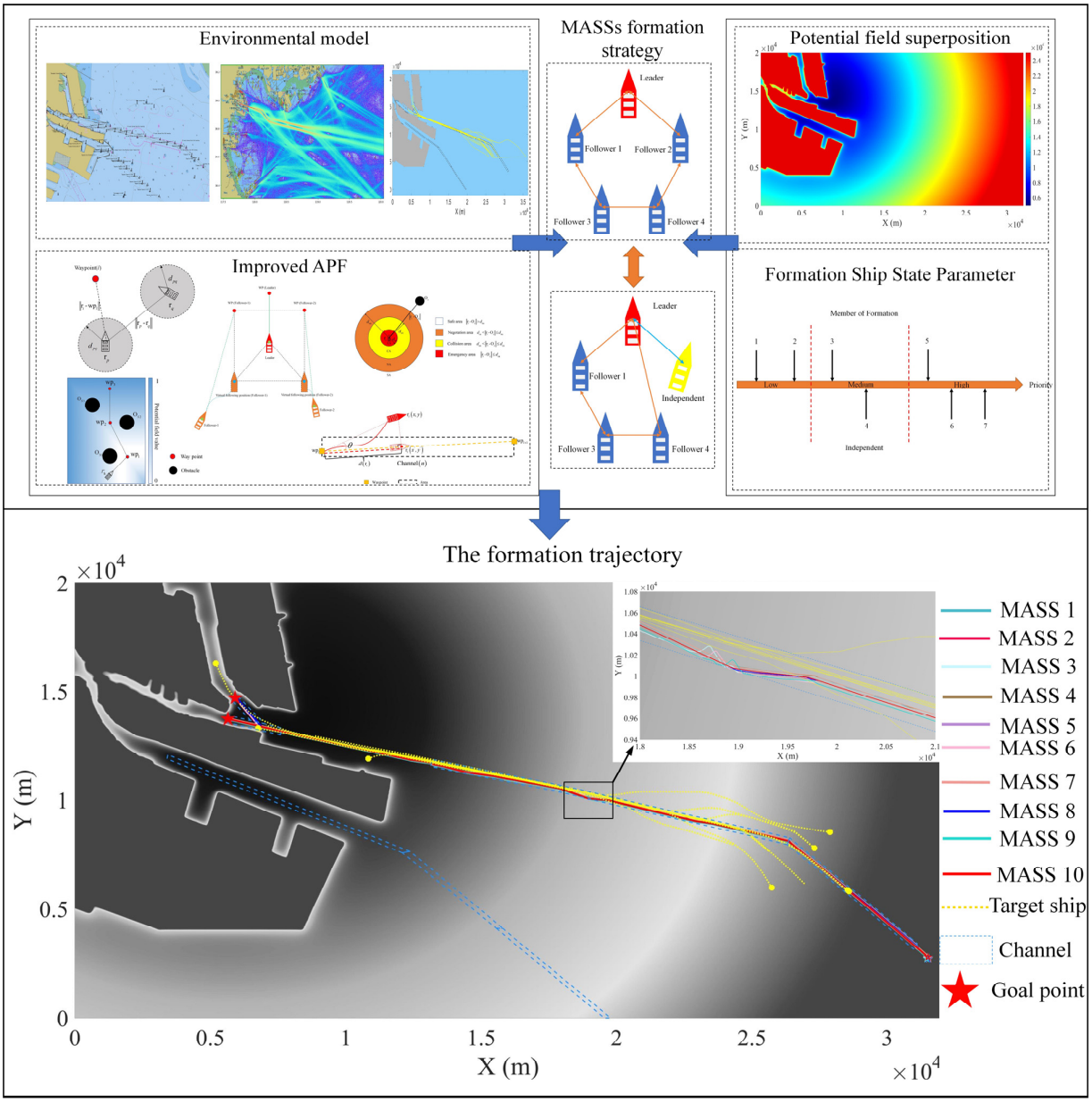

Figure 3. Full text structure diagram.

2. Problem Description

According to IMO's recent discussion on the coexistence of common ships and MASSs in highly interdependent systems, it can be inferred that the research trend of the MASS issue is as follows:

(1) Environmental modeling needs to consider the real navigation environment, as well as the channel systems of highly dependent interactions.
(2) The test should expand to multiple ships, and the test object should be F-MASSs.
(3) The situation of encountering a target ship (common ship) should be considered.
(4) The method should give real-time calculation results and return executable schemes.
(5) Real navigation data should be added for simulation test and verification.

The aim of this study is to design an algorithm that can consider some of the constraints faced by the development trend of F-MASSs and to propose a solution that satisfies the above constraints.

2.1. Assumptions

Since the middle of the last century, manned ships have gradually developed to become giant ships and super-large ships. The maximum length of traditional ships is close to 500 m, and the dead-weight tonnage (DWT) is more than 500,000. The emerging MASSs that do not need to keep a watch on the engine space have developed since the end of the last century, and the development of MASSs has gradually become popular in the last ten years. Both the length and load of MASSs have doubled, as shown in Table 1. Figure 4 shows the MASS/unmanned ship and manned ship size and DWT change.

Table 1. MASS (unmanned ship) and manned ship information (1975–2022).

Number	Name of Vessel	Time	Length Overall (LOA)	Dead-Weight Tonnage (DWT)	Manned/Unmanned
1	Berge Emperor	1975	333	211,360	M
2	Batillus	1976	381.82	554,000	M
3	Pierre Guillaumat	1977	399	555,000	M
4	Esso Atlantic	1977	400	500,000	M
5	Seawise Giant	1979	406.57	564,763	M
6	ARTEMIS	1993	1.37	0.2	U
7	ACES	1996	2.3	0.5	U
8	CARAVELA	1998	5	2	U
9	Spartan Scout	2001	11	4	U
10	USSV-HTF	2003	12	8.16	U
11	Xinpuyang	2010	414	350,000	M
12	X-2	2012	13	16	U
13	Protector Fifth	2012	15	26	U
14	Maersk Mc-Kinney Moller	2013	414.22	194,849	M
15	Prelude FLNG	2013	458.45	600,000	M
16	ACTUV	2015	19.1	157	U
17	CSCL Globe	2015	488	186,000	M
18	Sea Hunter	2016	40	145	U
19	Rolls Royce	2017	60	700	U
20	Folgefonn	2018	66	597	U
21	Yara Biekeland	2021	80	600	U
22	ASKO	2022	84.7	448	U
23	Zhuhai Cloud	2022	88.5	2000	U

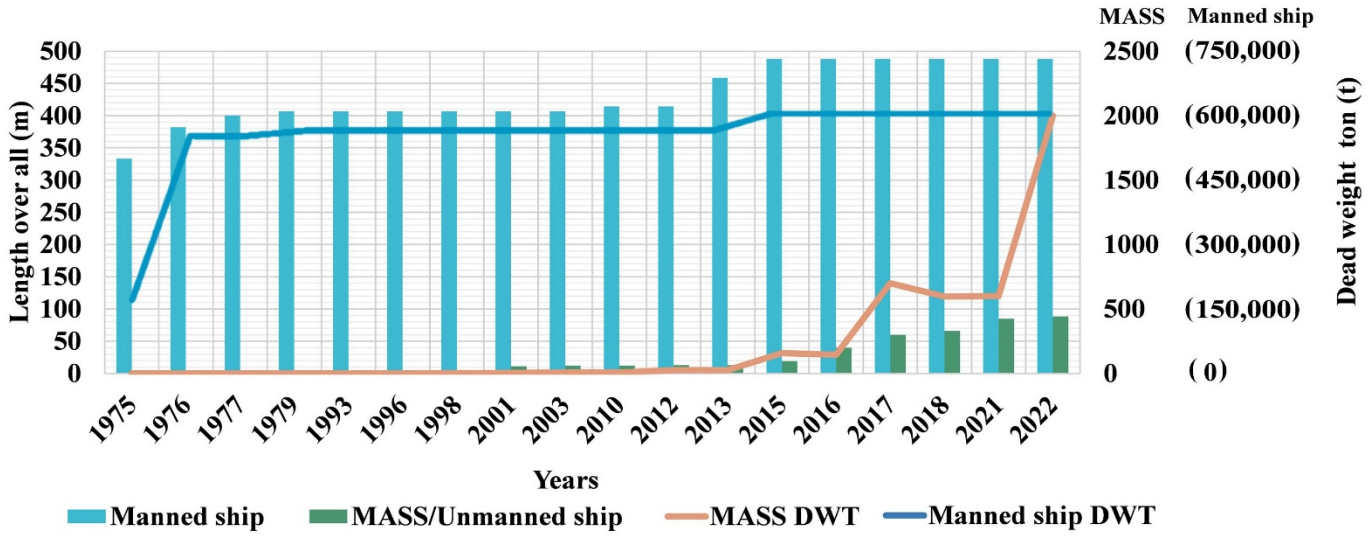

Figure 4. MASS (unmanned ship) and manned ship size change (1975–2022).

Before this paper introduces the relevant algorithms to satisfy the above requirements, some assumptions and constraints that should apply to MASSs are involved in this paper.

Static obstacles (land and islands) and the coordinates of the channel extracted from the S-57 ENC and the dynamic obstacles formed by target ship (common ship) replayed from AIS data constitute constraints in the process of MASS path following. When a MASS encounters common ships, CORLEGs do not make rules for the collision-avoidance actions of 'unmanned–manned' encounter situations. Therefore, according to the collision-avoidance regulations [34], "Under the maritime mode of unmanned-manned" situation:

1. The new requirement in Rule 18 has been proposed: "Under the maritime encounter mode of un-manned-manned, the level of MASS is lower than manned. A MASS underway shall keep out of the way of manned ship and a MASS shall not impede the passage of any other manned navigating vessels." A MASS underway shall keep out of the way of: (i) a power-driven vessel; (ii) a vessel not under command; (iii) a vessel restricted in her ability to maneuver; (iv) a vessel engaged in fishing; (v) a sailing vessel;
2. Because the maneuverability of a MASS far exceeds that of manned vessels, in order to pursue the efficiency of autonomous navigation of MASS, this study assumes that MASS does not apply to Rule 16 in the COLREGs: "take early, substantial action, so far as possible and keep well clear".

According to the above two regulations, under the 'unmanned–manned' encounter situation, MASS should give way to five kinds of ships. Extended to F-MASSs, the formation should give way to the five prescribed kinds of ships.

The following assumptions are considered in the MASS path-following algorithm:

- MASS safe path means that the line from the preset destination to the current ship position does not intersect with any obstacles;
- MASS is regarded as a moving point with ship domain;
- The trajectory of the target ship will not be affected by the MASS, and target ship will keep its heading and speed;
- The speed and heading of the MASS are controlled by the potential field.

2.2. Formation Strategy

In the navigation process of F-MASSs, how ships communicate with each other and how to deliver instructions are the first problems to be solved. In this paper, the formation strategy based on Leader–Follower was adopted, and the topology structure was appropriately improved according to the formation situation in the environment. The leader–follower strategy entails that one object is selected as the leader of the formation, and other objects generate guidance waypoints according to the identity of the followers, and the followers feed back to the leader in real time to verify the stability of the formation structure.

Therefore, on the basis of the Leader–Follower strategy, in addition to the identities of the leader and followers, a new identity was defined as being the independent ship. When a member ship is affected by a constraint condition, it is temporarily separated from the formation to remove the constraint and return to the formation once the situation is solved. In general, the formation adopts a fixed Leader–Follower strategy as shown in Figure 5a The global information is shared by the leader and followers, which can transmit information to each other. However, when some ships in the formation need to leave the original formation temporarily to deal with abnormal constraint conditions due to external factors, the formation strategy is transformed into a variable Leader–Follower, as shown in Figure 5b, and the yellow ship's identity is independent; it is separated from the original formation temporarily. At this time, the leader communicates with the independent ships and reserves its position in the formation. The independent ship returns to the original formation after dealing with the abnormal constraint condition. In F-MASSs, each ship's task may be different, and the formation pattern is adjusted by instant communication

among ships, according to the variable structure Leader–Follower strategy, each MASS as a control object with the unique expectation path. The desired path of the followers is generated by the trajectory of the leader and its relative position.

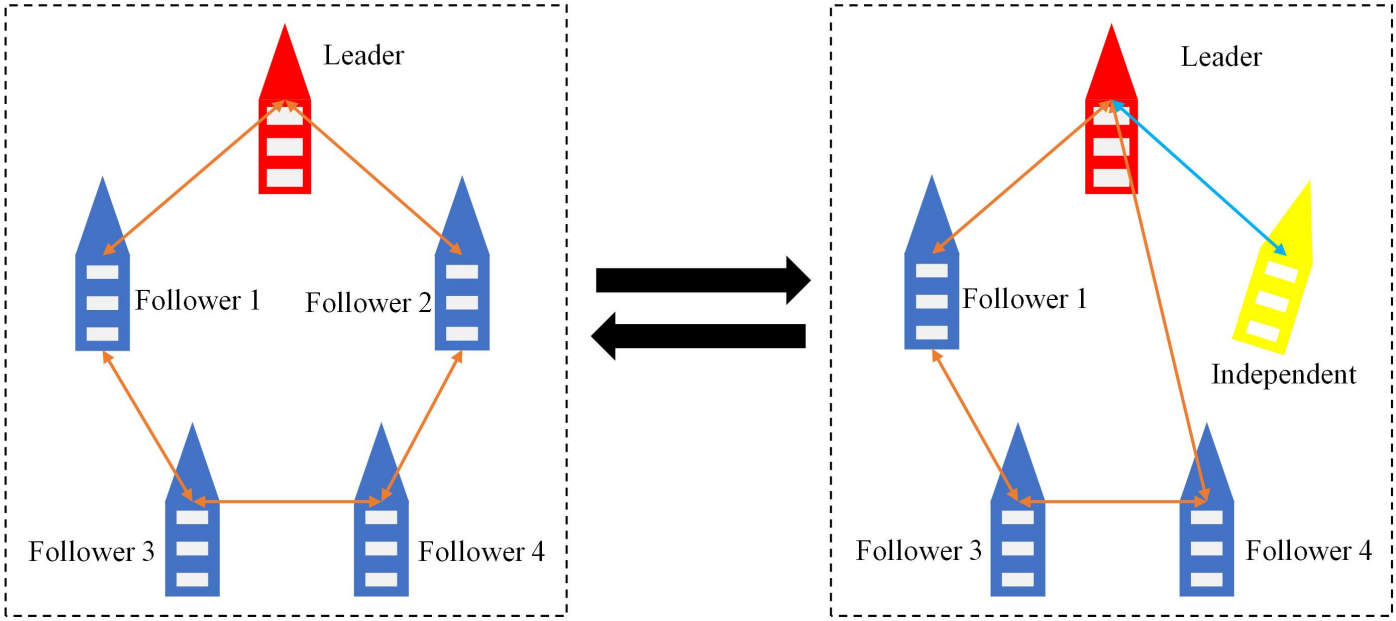

Figure 5. Strategy of Leader–Follower.

3. Methodology

Path planning refers to finding the path of moving objects from the starting point to the destination to avoid collisions with static and dynamic obstacles in the environment. The final path is the result of reaching an equilibrium with multiple constraints. The path that can pass from the starting point to the destination without intersecting any obstacles is called a collision-free path.

3.1. Definition of Formation Ship State Parameter

The purpose of MASS path planning is to find a safe trajectory between the initial position of the MASS and the destination in a specific navigation environment and realize the path following under a set of multiple constraints. Many people have conducted extensive research on path planning. However, when the F-MASSs are constrained in a constrained environment, it is very challenging for the F-MASSs to sail in the constrained environment compared with the open water. Although the possible interference effects of land and wrecks and other obstacles are avoided as much as possible through the set formation path in the channel in advance, it also puts the F-MASSs in the situation of sailing together with common ships in the same narrow water area. The path, under the constraints of the channel and the influence of target ships (common ships), is followed by the F-MASSs. Therefore, the Formation Ship State Parameters (FSSPs) of the F-MASSs are defined in advance, and the tasks being executed by each MASS are known by the FSSP values marked on every MASS. The decisions suitable for the current environmental conditions are generated for each ship according to the FSSP.

During navigation, a member in the formation is separated from the main formation due to a static obstacle, target ship's influence, formation pattern change, restricted channel area, or other factors. At this time, because each MASS has different FSSPs, each ship needs to be handled differently for different cases. Considering the good maneuverability and

fast response of the MASS, the following formula (Equations (1)−(6)) of the MASS divides the states the MASS encounters into different situations during navigation.

$$\mathrm{PE_{MASS}} = \mathrm{PE_{goal}} + \mathrm{PE_{obs}} + \mathrm{PE_{FS}} + \mathrm{PE_{TS}} + \mathrm{PE_{cha}}, \tag{1}$$

$$\mathrm{PE_{goal}} = \sum \mathrm{U}^{\mathrm{wp}_l} \; l \in I_{\mathrm{wp}}, \tag{2}$$

$$\mathrm{PE_{obs}} = \sum \mathrm{U}^{\mathrm{obs}_s} \; s \in I_{\mathrm{obs}}, \tag{3}$$

$$\mathrm{PE_{FS}} = \sum \mathrm{U}^{\mathrm{FS}_i} \; i \in I_{\mathrm{FS}}, \tag{4}$$

$$\mathrm{PE_{TS}} = \sum \mathrm{U}^{\mathrm{m}_k} \; k \in I_{\mathrm{m}}, \tag{5}$$

$$\mathrm{PE_{cha}} = \begin{cases} 0 & (x,y) \in \mathrm{Area(channel)} \\ \sum \mathrm{U}^{\mathrm{cha}_n} & (x,y) \notin \mathrm{Area(channel)} \end{cases} n \in I_{\mathrm{cha}}, \tag{6}$$

$\mathrm{PE_{MASS}}$ represents the total potential energy of each MASS; $\mathrm{PE_{MASS}}$ represents the goal point of the potential energy; $\mathrm{U}^{\mathrm{wp}_l}$ represents the waypoint l potential value; I_{wp} is the set of waypoints; $\mathrm{PE_{obs}}$ represents the obstacle's potential energy; $\mathrm{U}^{\mathrm{obs}_s}$ represents the obstacle's potential value; I_{obs} is the set of obstacles; $\mathrm{PE_{FS}}$ represents the other MASS influence of the potential energy of the formation; $\mathrm{U}^{\mathrm{FS}_i}$ represents the MASS number of i generated of the potential value; I_{FS} is the set of formation; $\mathrm{PE_{TS}}$ represents the target ship's (common ship) influence of the potential energy; $\mathrm{U}^{\mathrm{m}_k}$ represents the target ship's potential value; I_{m} is the set of target ships; $\mathrm{PE_{cha}}$ represents the channel's potential energy; $\mathrm{U}^{\mathrm{cha}_n}$ represents the channel number n of the potential value; I_{cha} is the set of channel area.

We summarized waypoints, obstacles, target ships, formation ships, and channel potential energy values in order to make the MASS conform to the FSSP in action and set the priority of different types of FSSPs. Table 2 gives the detailed information and priority of each FSSP, and the more explicit FSSP is given by Figure 6. The condition of the MASS being underway is throughout the entire navigation process, but it is also the lowest priority. As long as $\mathrm{PE_{goal}} > 0$, the MASS will continue to sail. The higher priority level means that when the above constraints restrict the MASS, the MASS will give priority to take actions that meet the higher priority constraints. The constraint of $\mathrm{PE_{cha}}$ means that as long as the current position of the MASS is in the area of the channel, the constraint will not take effect, otherwise the MASS is attracted to the channel. By setting the priority for different constraints, the F-MASSs can prioritize the constraints that have a high-priority impact and then resolve the other lower-priority constraints separately. When $\mathrm{PE_{MASS}} = 0$, all the known constraints have no effect, and the MASS navigation process is accomplished.

Table 2. MASS (unmanned ship) Formation Ship State Parameter.

Condition Number	Formation Ship State Condition	Priority	Independent from Formation (Yes/No)
1	Underway	Low	N
2	Goal arrived	Low	N
3	Static obstacle influence	Medium	N
4	Out of channel	Medium	Y
5	Other MASS influence	High	N
6	Encounter single manned ship	High	Y
7	Encounter two or more manned ships	High	Y

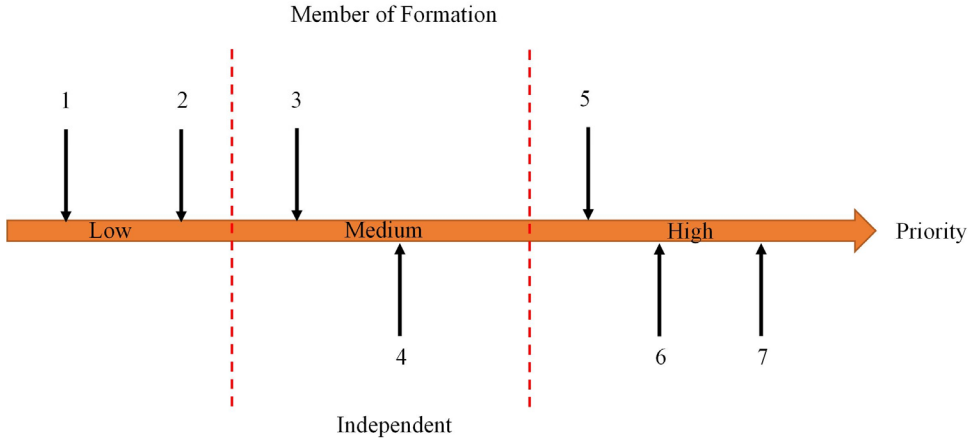

Figure 6. Priority of FSSP.

3.2. Path following by Improved APF

APF is a widely used method in the field of agent path following. Through the construction of potential function, the agent is affected by the potential field around the obstacles in the navigation process, and the agent moves away from obstacles and continues to be near the goal position under the influence of the potential field. The traditional APF method is suitable for the path following of a single ship, but F-MASS contains many ships. The formation is treated as the smallest unit, the traditional APF method could not satisfy the constraints, such as the influence of waypoint to F-MASS, target ship and static obstacles to F-MASSs, channel area to F-MASSs, and internal ship interaction to F-MASS.

In order to ensure that F-MASS is consistent with the preset path as much as possible in the path-following process, an improved APF model was proposed. This model is applicable to the path following of F-MASS under multiple constraints, and it makes the Leader–Follower strategy suitable for the path-following process.

The MASS motion model is the kinematic model, described by the following Equation (7):

$$\begin{cases} x_{j+1}^{\mathrm{r}_i} = x_j^{\mathrm{r}_i} + v_j^{\mathrm{r}_i}\delta t\cos\theta_j^{\mathrm{r}_i} \\ y_{j+1}^{\mathrm{r}_i} = y_j^{\mathrm{r}_i} + v_j^{\mathrm{r}_i}\delta t\sin\theta_j^{\mathrm{r}_i} \\ \theta_{j+1}^{\mathrm{r}_i} = \theta_j^{\mathrm{r}_i} + \omega_j^{\mathrm{r}_i}\delta t \end{cases} \quad i \in I_{\mathrm{R}}, j \in T \tag{7}$$

where j represents the time of iterations; it is contained in total time T; r_i represents the serial number of MASS; δt represents the counting period of adjacent iteration; and I_{R} represents the F-MASSs.

In each iteration period, the positions and directions of each MASS are changed. With the potential field formed by the superposition of waypoints and obstacles, the tasks of switching waypoints, avoiding static and dynamic obstacles, staying in the channel area, and maintaining the formation shape are required for F-MASS in path following. Therefore, the APF method applicable to multiple ships was improved as follows (Equations (8)−(13)):

$$U_{\mathrm{r}_p}^{\mathrm{r}_q}(\mathrm{r}_p,\mathrm{r}_q) = \begin{cases} \sum_{q\neq p}^{N}\left(\eta_{11}\left(\frac{1}{\|\mathrm{r}_p-\mathrm{r}_q\|}-\frac{1}{d_{pq}}\right)\frac{1}{\|\mathrm{r}_p-\mathrm{r}_q\|^2}\|\mathrm{r}_p-\mathrm{wp}_l\|^2+\eta_{12}\left(\frac{1}{\|\mathrm{r}_p-\mathrm{r}_q\|}-\frac{1}{d_{pq}}\right)^2\|\mathrm{r}_p-\mathrm{wp}_q\|^2\right) & \|\mathrm{r}_p-\mathrm{wp}_l\|<d_{pq} \\ 0 & \|\mathrm{r}_p-\mathrm{wp}_l\|\geq d_{pq} \end{cases} \quad p,q\in I_{\mathrm{R}}, l\in I_{\mathrm{wp}} \tag{8}$$

$$U_{\mathrm{r}_h}^{\mathrm{wp}_l}(\mathrm{r}_h,\mathrm{wp}_l) = \eta_{21}\|\mathrm{r}_h-\mathrm{wp}_l\| \; h\in I_{\mathrm{R}}, l\in I_{\mathrm{wp}} \tag{9}$$

$$U_{\mathrm{r}_i}^{\mathrm{r}_{hi}}(\mathrm{r}_i,\mathrm{r}_{hi}) = \eta_{22}\|\mathrm{r}_i-\mathrm{r}_{hi}\| \; i\in I_{\mathrm{R}}, h\in \mathrm{I}_{\mathrm{R}} \tag{10}$$

$$U_{\mathrm{r}_i}^{\mathrm{m}_k}(\mathrm{r}_i,\mathrm{m}_k) = \sum_{k=1}^{I_{\mathrm{m}}}\eta_3\left(d_{\mathrm{rep}}-\|\mathrm{r}_i-\mathrm{m}_{k,I_{\mathrm{m}}}\|\right)^2 \; 0<\|\mathrm{r}_i-\mathrm{m}_{k,I_{\mathrm{m}}}\|\leq d_{\mathrm{rep}}, i\in I_{\mathrm{R}}, k\in I_{\mathrm{m}} \tag{11}$$

$$U_{r_i}^{O_s}(r_i, O_s) = \begin{cases} \eta_{41}\left(\frac{1}{\|r_i - O_s\|} - \frac{1}{d_{na}}\right)\frac{1}{\|r_i - O_s\|^2}\|r_i - wp_l\|^2 + \eta_{42}\left(\frac{1}{\|r_i - O_s\|} - \frac{1}{d_{na}}\right)^2\|r_i - wp_l\| & d_{ca} < \|r_i - O_s\| \le d_{na} \\ \eta_{41}\left(\frac{1}{\|r_i - O_s\|} - \frac{1}{d_{ca}}\right)\frac{1}{\|r_i - O_s\|^2}\|r_i - wp_l\|^2 + \eta_{43}\left(\frac{1}{\|r_i - O_s\|} - \frac{1}{d_{ca}}\right)^2\|r_i - wp_l\| & d_{ea} < \|r_i - O_s\| \le d_{ca} \\ \eta_{41}\left(\frac{1}{\|r_i - O_s\|} - \frac{1}{d_{ea}}\right)\frac{1}{\|r_i - O_s\|^2}\|r_i - wp_l\|^2 + \eta_{44}\left(\frac{1}{\|r_i - O_s\|} - \frac{1}{d_{ea}}\right)^2\|r_i - wp_l\| & \|r_i - O_s\| \le d_{ea} \end{cases} \quad i \in I_R, s \in I_O, l \in I_{wp} \tag{12}$$

$$U_{r_i}^{C_n}(r_i, C_n) = \begin{cases} \eta_5\|(\|r_i - wp_l\| \cdot \cos\theta + wp_l) - r_i\| & r_i(x,y) \notin \text{Area}(\text{cha}[n]) \\ 0 & r_i(x,y) \in \text{Area}(\text{cha}[n]) \end{cases} i \in I_R, l \in I_{wp}, n \in I_C \tag{13}$$

$\eta_{11}, \eta_{12}, \eta_{21}, \eta_{22}, \eta_3, \eta_{41}, \eta_{42}, \eta_{43}, \eta_{44}$ and η_5 represent the positive calibration constant of the corresponding potential function.

Equation (8) represents the potential field function of the MASS inside the formation, and d_{pq} represents the ship domain of the MASS. As long as $\|r_p - r_q\| > d_{pq} \forall p, q \in I_R$, the condition between MASS-p and MASS-q is relatively safe. If the distance norm is 0, the potential field value becomes infinite. Figure 7 represents the calculation of repulsion between MASS-p and MASS-q.

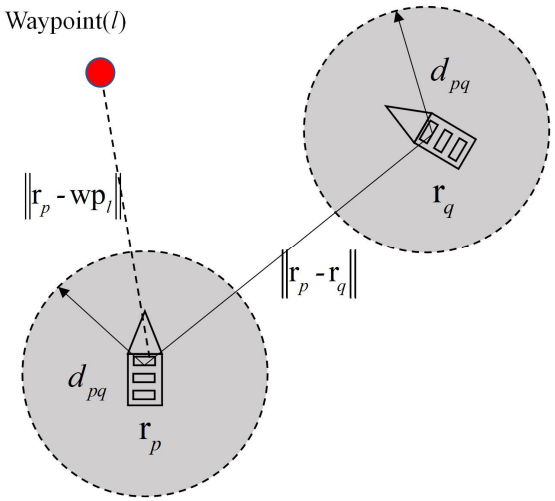

Figure 7. Calculation of the repulsion force between MASS-p and MASS-q.

In Equation (9), r_h represents the leader and is not affected by other MASSs in the formation. wp_l represents the destination of the path segment and belongs to $I_{wp} = \{1, 2, \ldots, G_{wp}\}$, as shown in Figure 8 The waypoint has the gravitational potential field for MASS and will be switched to the next waypoint when the MASS arrives nearby. $U_{r_h}^{wp_l}$ represents the gravitational potential energy of the leader subjected to the waypoint.

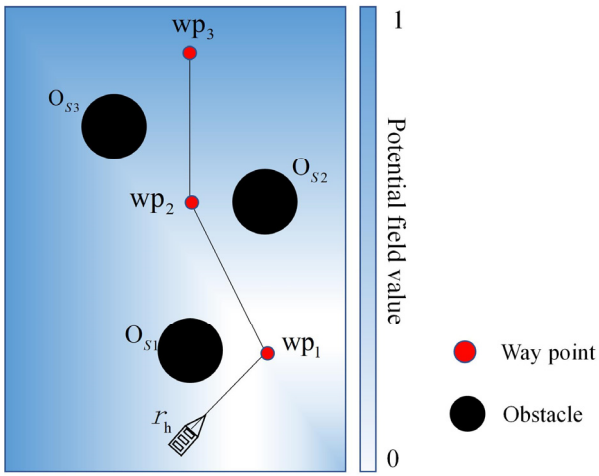

Figure 8. Process of leader ship passing through multiple waypoints.

As Figure 9 shows, a formation is formed with a leader and two followers. The corresponding waypoints (red points) in the path are set to each ship. The blue points represent the virtual following positions set by the leader to each follower. In the process of navigation, the follower is affected by the gravitational potential field generated by the virtual following position, and the virtual following position is updated by the position of the leader.

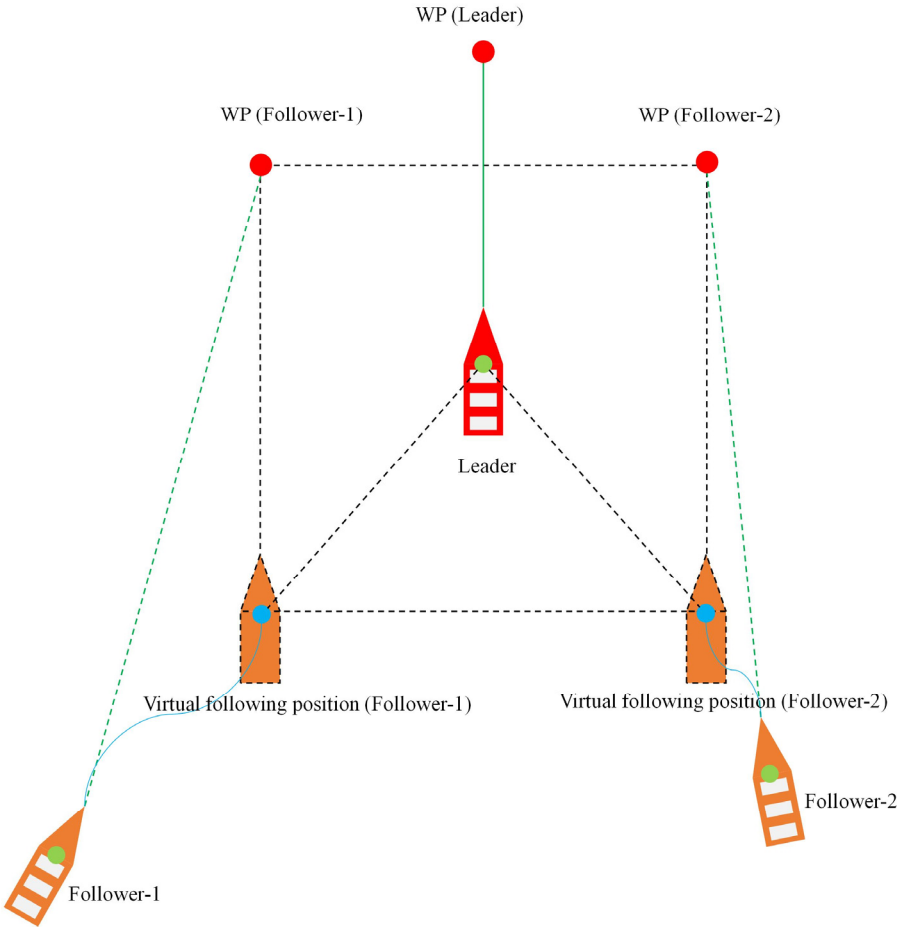

Figure 9. Follower and leader relationship in formation.

Equation (11) considers the influence of dynamic obstacles (target ships) repulsion potential field on the formation; $U_{\mathrm{r}_i}^{\mathrm{m}_k}$ refers to the potential energy of the MASS entering the influence range of dynamic obstacles, which contains dynamic obstacles within the distance range $0 < \|\mathrm{r}_i - \mathrm{m}_{k,I_\mathrm{m}}\| \leq d_{\mathrm{rep}}$; d_{rep} represents the maximum impact distance of dynamic obstacles.

In Equation (12), $U_{\mathrm{r}_i}^{\mathrm{O}_s}$ represents the repulsion potential field of MASS affected by static obstacles O_s. As shown in Figure 10, according to the distance between the obstacle and the MASS, the influence can be divided into three stages, that is, the negotiation area $d_{\mathrm{ca}} < \|\mathrm{r}_i - \mathrm{O}_s\| \leq d_{\mathrm{na}}$, the collision risk area $d_{\mathrm{ea}} < \|\mathrm{r}_i - \mathrm{O}_s\| \leq d_{\mathrm{ca}}$, and the emergency risk area $\|\mathrm{r}_i - \mathrm{O}_s\| \leq d_{\mathrm{ea}}$. The hierarchical collision-avoidance function can lead to different collision-avoidance actions and improve the priority of obstacle avoidance according to the risk level of the MASS and the obstacles.

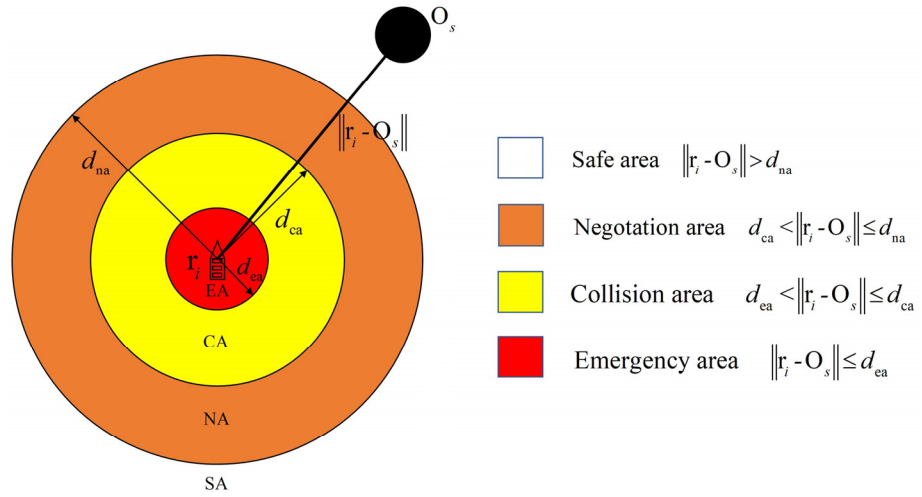

Figure 10. Types of collision-avoidance actions with the distance between obstacles and MASS (unmanned ship).

In Equation (13), $U_{r_i}^{C_n}$ represents the potential value of MASS in the corresponding channel, and it is necessary to determine whether the position of MASS is within the current channel segment. As shown in Figure 11, if the MASS position is not in the channel segment, the virtual MASS ship position is generated by the channel constraint and the MASS position, and the MASS is affected by the channel's potential field. The virtual MASS position is determined according to the proportion of the MASS's distance in the current channel path. The MASS is given gravitational potential energy to push it back into the channel.

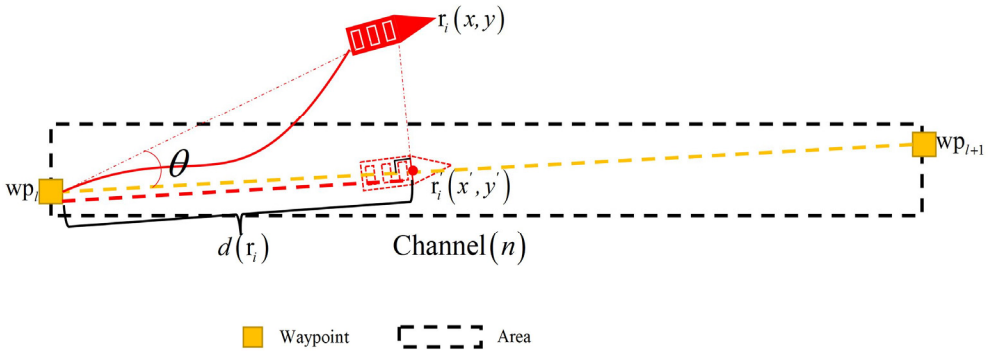

Figure 11. Projection position of MASS (unmanned ship) in the channel.

Based on the formulas, a multiple-constraint APF model for F-MASSs was established, which can assist F-MASSs to complete path following.

When the F-MASS is in a restricted area, the leader of the formation is the master. Each follower's waypoint is set by the leader. The follower is attracted by a virtual following position, which is generated by the leader with the FSSP status of underway, forming a fixed Leader–Follower structure. At this time, the formation is divided into leader and followers. According to the switch of the ship's FSSP, some MASSs need to deal with different tasks, and the formation is a variable Leader–Follower structure.

Figure 12 shows the information framework of the formation. The F-MASS's preset path is set by the environmental map model. The leader can sense the information of static obstacles, target ships, and boundary information of the channel and share it with other followers in the formation. If there is a ship FSSP change in the formation, its identity is transformed into an independent ship. The 'unmanned–manned' rules or channel area information accordingly are considered by the independent ship, and after its FSSP status changes to underway, it can return to the original formation. The information of static

obstacles, target ships, and channel areas and formation ship positions is shared by the general leader and the independent ship.

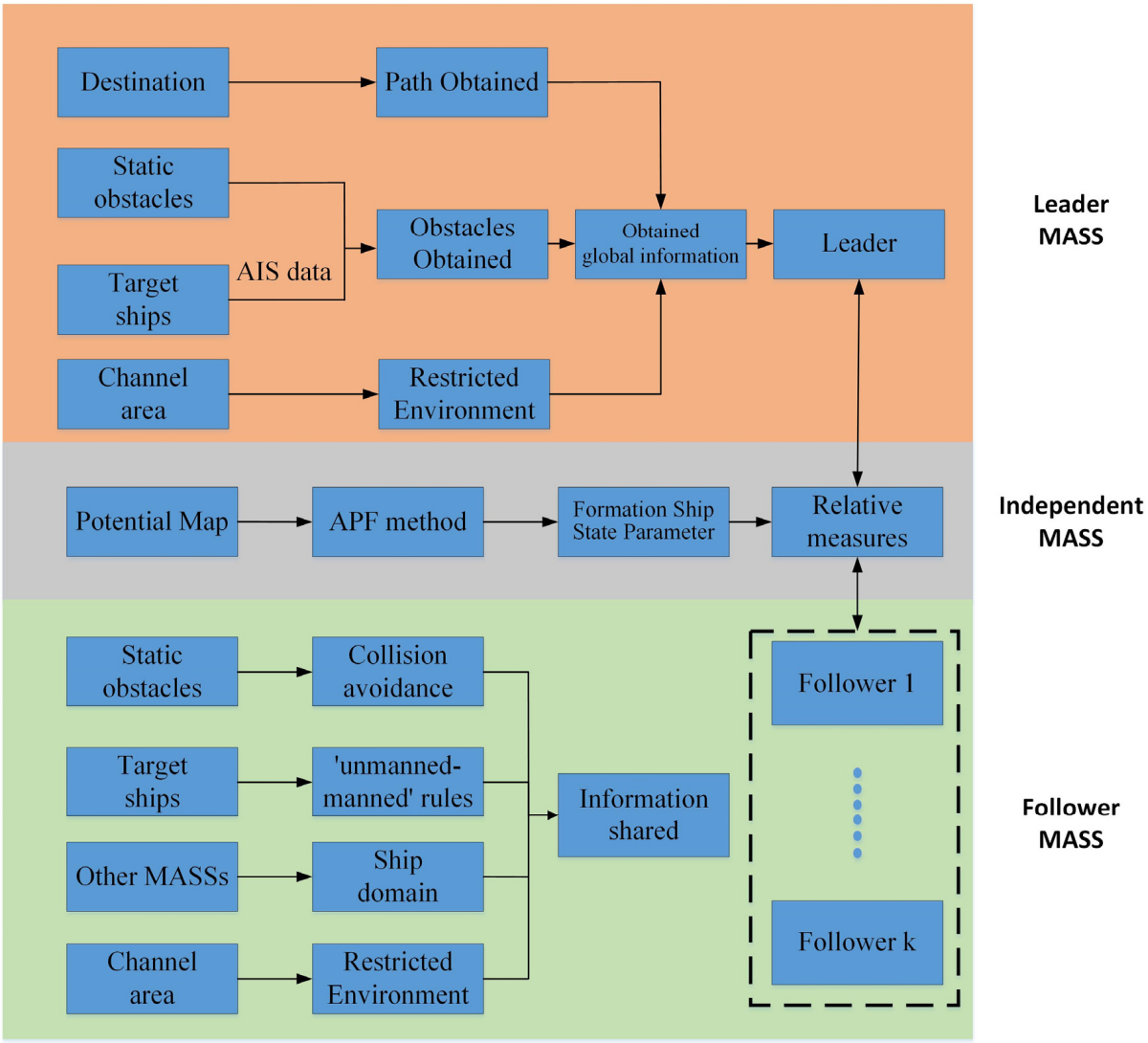

Figure 12. Formation information framework.

4. Results

In order to verify whether the F-MASS can be used in multiple constrained environments, the path-following test under the formation conditions was verified by the improved APF method. According to the two types of Leader–Follower strategies, the formation transformation was realized in the simulation process, and a series of simulations were performed on the MASS under the assumed conditions.

In this study, AIS data near Tianjin Port in 2018 were used. Figure 13. shows the AIS big data trajectory of the ship near in Tianjin Port. In order to achieve the smooth display of the AIS data in the experiment, the AIS data with different recording intervals were interpolated. Table 3 shows the Maritime Mobile Service Identity (MMSI), navigation time, and start and end positions of the nine target ships.

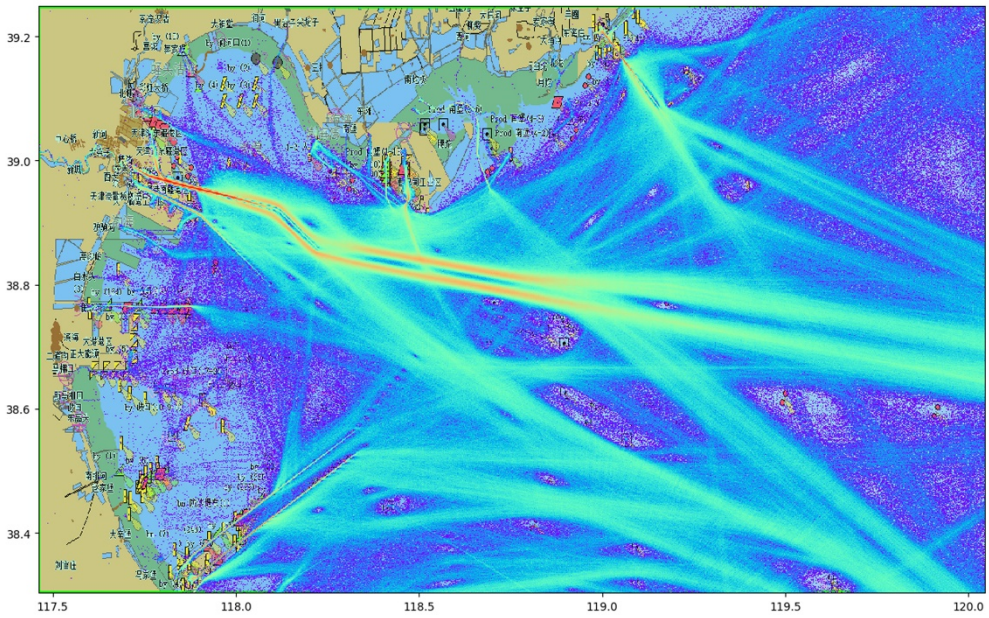

Figure 13. AIS big data in Tianjin Port.

Table 3. Information of target ships.

Number	MMSI	Time (s)	St Lon (°)	St Lat (°)	End Lon (°)	End Lat (°)
1	412324XXX	955326	118.193163	38.921905	118.121075	38.900713
2	413009XXX	5839	117.807897	38.966292	118.116877	38.90437
3	205535XXX	174692	118.152903	38.898737	118.108925	38.899028
4	210744XXX	9557	118.162478	38.900607	117.764168	38.974515
5	211781XXX	92198	118.132792	38.91676	118.134378	38.89856
6	215040XXX	276964	118.151967	38.899352	118.127538	38.899588
7	215049XXX	4029	117.872245	38.95363	118.128385	38.901042
8	220478XXX	5896	117.783103	38.993058	118.135603	38.897817
9	228354XXX	88613	118.132833	38.916667	118.124833	38.8985

Before the simulation test, the potential environmental field model, including obstacles, target ships, channel areas, and F-MASSs, was first established. The establishment of the environmental model included the extraction and description of characteristic environmental information. Electronic navigation charts store relevant elements in data files in geometric forms, such as points, lines, and planes, and can display and select and relevant navigational and environmental information required by adjusting the number of layers. It is the basis of the navigation environment model to read the S-57 data packet information of the test area and screen out relevant land and channel information. Due to the uneven distribution of land and the complex structure of obstacles in the selected environment, it took a lot of calculating to refine the corresponding terrain coordinates, so the boundary points of the obstacles were selected as the feature coordinates for extraction, and the boundary points with large spacing were interpolated. As shown in Figure 14, (a) is the original information of the S-57 Electronic Navigation Chart of Tianjin Port. (b) is the environmental model after extracting the coordinates of AIS data, land, and channel areas in the set area. (c) is the value of the gravitational potential field at the goal. (d) is the under the obstacle influence of the superposition potential field.

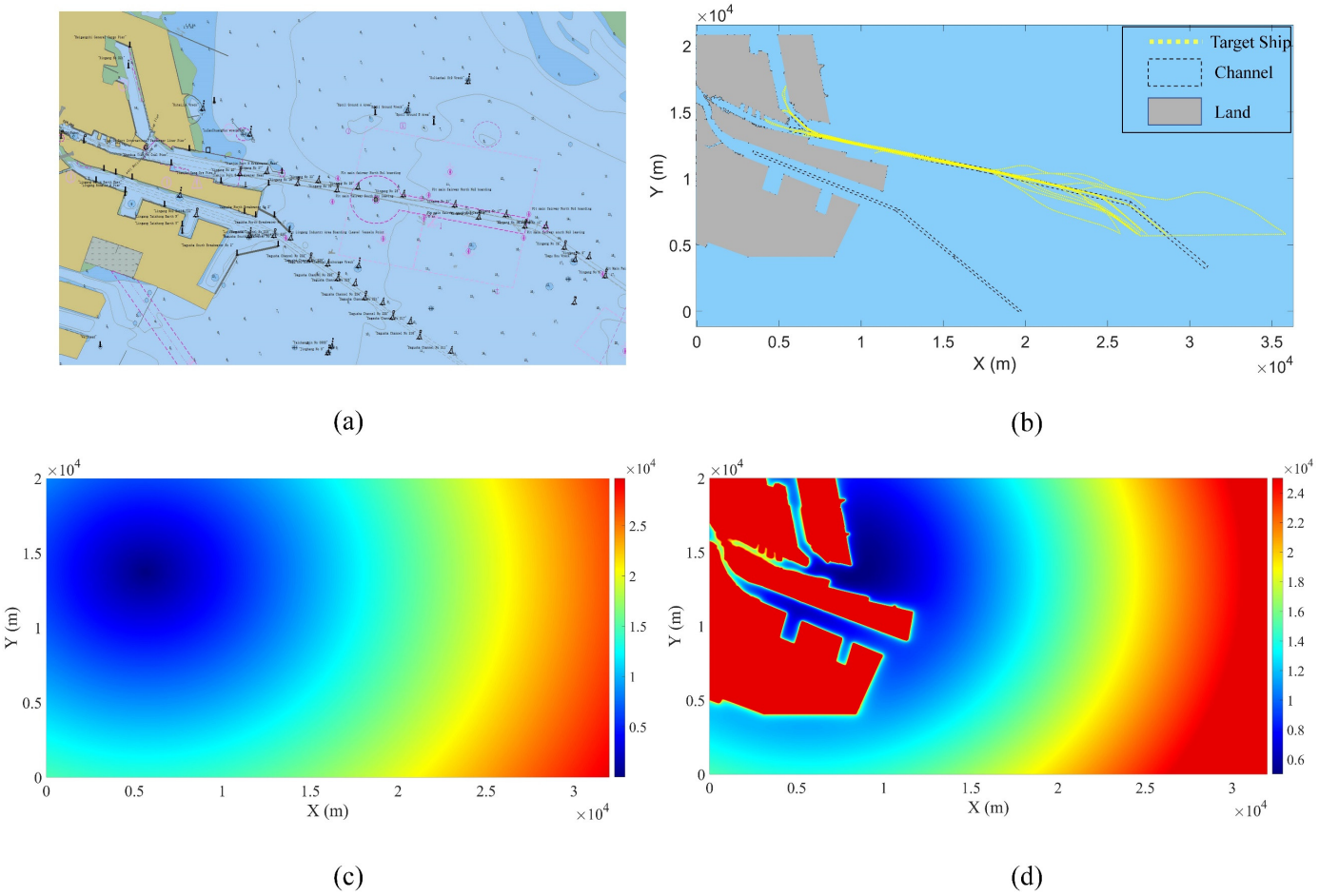

Figure 14. (**a**) Electronic navigational chart of Tianjin Port; (**b**) extraction of target ship trajectory, land and channel areas; (**c**) gravitational potential field; and (**d**) superposition potential field.

The main channel of Tianjin Port was selected as the preset path of the F-MASSs, and waypoints were set for the F-MASSs at the beginning and end of each channel to ensure that the formation was always sailing in the channel area. During the sailing process of F-MASSs, each ship decided the action in the next iteration according to its own FSSP. As shown in Figure 15, the simulation process of the F-MASSs was recorded by time series. The entire simulation process was 5247 s long, and (b)–(f) represent an interval of 650 s. The yellow line is the trajectory of the target ships; the pink dashed line is the channel area, and the black is the obstacle. (a) shows the whole navigation process of the F-MASSs, and (b) shows that the F-MASSs entered the first section of the channel, and some target ships also began to move along the set path. In the process from (c) to (d), the F-MASSs entered the new channel segment. In the process of (e)–(f), the F-MASSs encountered TS-1 and conducted collision avoidance according to the 'unmanned-manned' encounter regulations. Some MASSs temporarily exceeded the channel due to collision avoidance. After the risk of collision avoidance with TS-1 was eliminated, the ship returned to the channel in time according to the constraints of the channel on the MASS. (h) shows that the F-MASSs was not restricted by the channel for the time being, which was decided according to the actual situation of the channel setting in Tianjin Port. In (i), the F-MASSs encountered the crossing channel. According to the goal set, the F-MASSs divided into two subformations, and each formation maintained the formation pattern of the subformation to reach the set goal point.

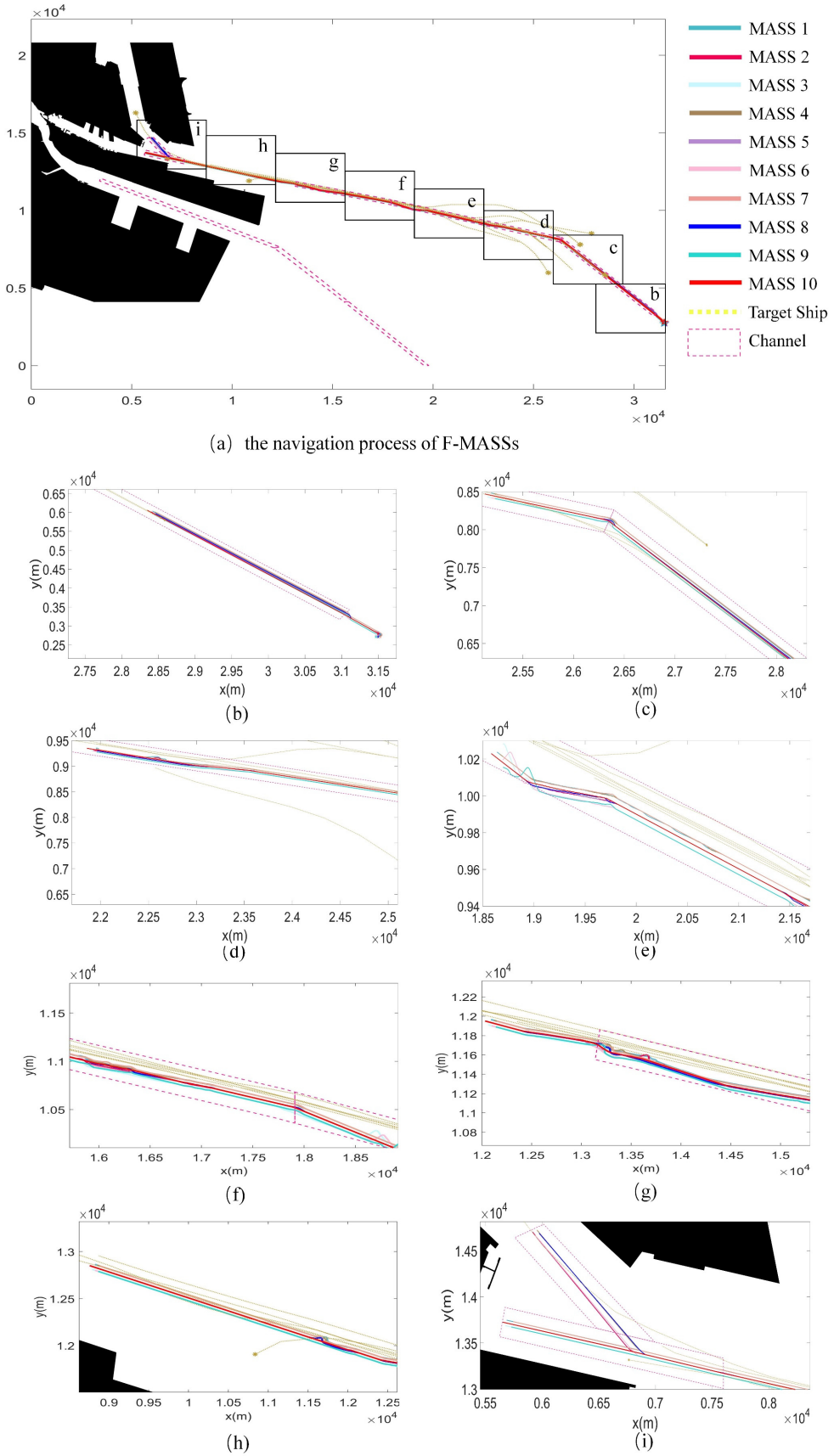

Figure 15. Time-specific marching diagram of formation, (**a**) is the navigation process of formation, (**b**–**i**) are the enlarged view of each period.

Figure 16 shows the process of the F-MASSs encountering one target ship, and the F-MASSs eliminated the risk of collision according to multiple constraints. (a) shows that the F-MASSs was about to form an 'unmanned–manned' cross encounter situation with TS-1, and when the MASS entered the ship domain of TS-1, the collision risk of the unmanned–manned ships was calculated. (b) shows that according to the risk assessment, the FSSP of the F-MASSs was changed to 'Encounter single manned ship'. The speed and heading of the F-MASSs were changed by the influence of TS-1. (c) shows that three MASSs trajectory were out of the channel due to collision avoidance with TS-1. Their condition was transformed into 'Out of channel', and these MASSs returned to the channel in time. (d) When the collision-avoidance action of the TS-1 was completed, the F-MASSs restored the formation pattern. (d) and (e) are the speed and heading changes of each ship in the formation during the collision-avoidance process.

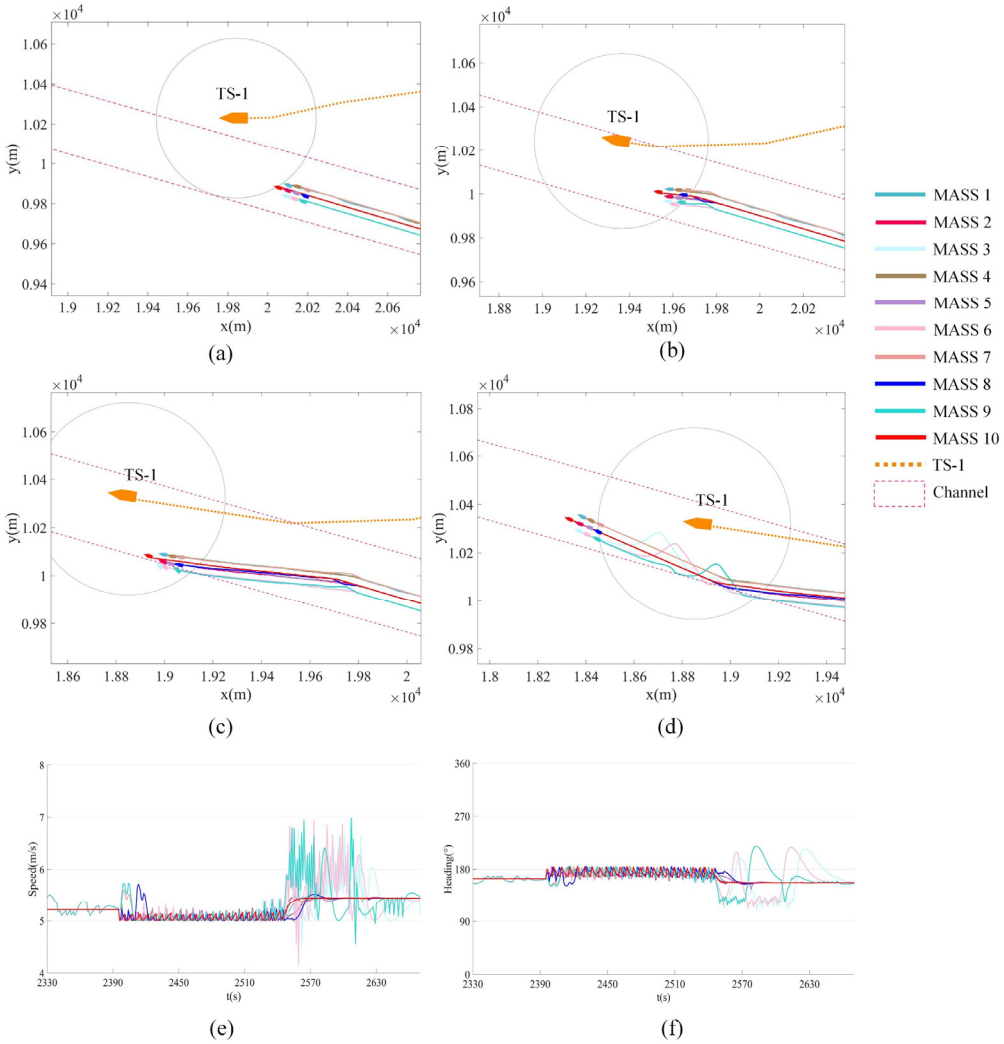

Figure 16. MASSs formation encountered one target ship situation. (**a**) About to form an encounter situation. (**b**) Gave way to TS-1. (**c**) Some MASSs went out of channel and returned to channel. (**d**) Avoidance completion of encounter situation to adjust formation pattern. (**e**) The MASS speed change during the situation. (**f**) The MASS heading change during the situation.

Figure 17 shows the process of the F-MASSs when encountering two target ships. (a) shows that the F-MASSs was about to form 'unmanned–manned' encounter situations with TS-3 and TS-5, and when the F-MASSs met two manned ships, the MASSs would give way to the ship with the shorter distance to them. (b) TS-3 ship had a higher priority to be given way than TS-5, and the MASSs took collision-avoidance action to TS-3 firstly, and the

FSSP of the F-MASSs was changed to 'Encounter two or more manned ships. The speed and heading of F-MASSs were changed by the influence of TS-3. (c) shows that when there was no collision risk between the F-MASSs and TS-3, the collision-avoidance action to TS-3 was completed and then to TS-5. (d) With collision-avoidance action of the two manned ships completed, the F-MASSs restored the formation pattern. (d) and (e) are the speed and heading changes of each ship in the formation during collision-avoidance process.

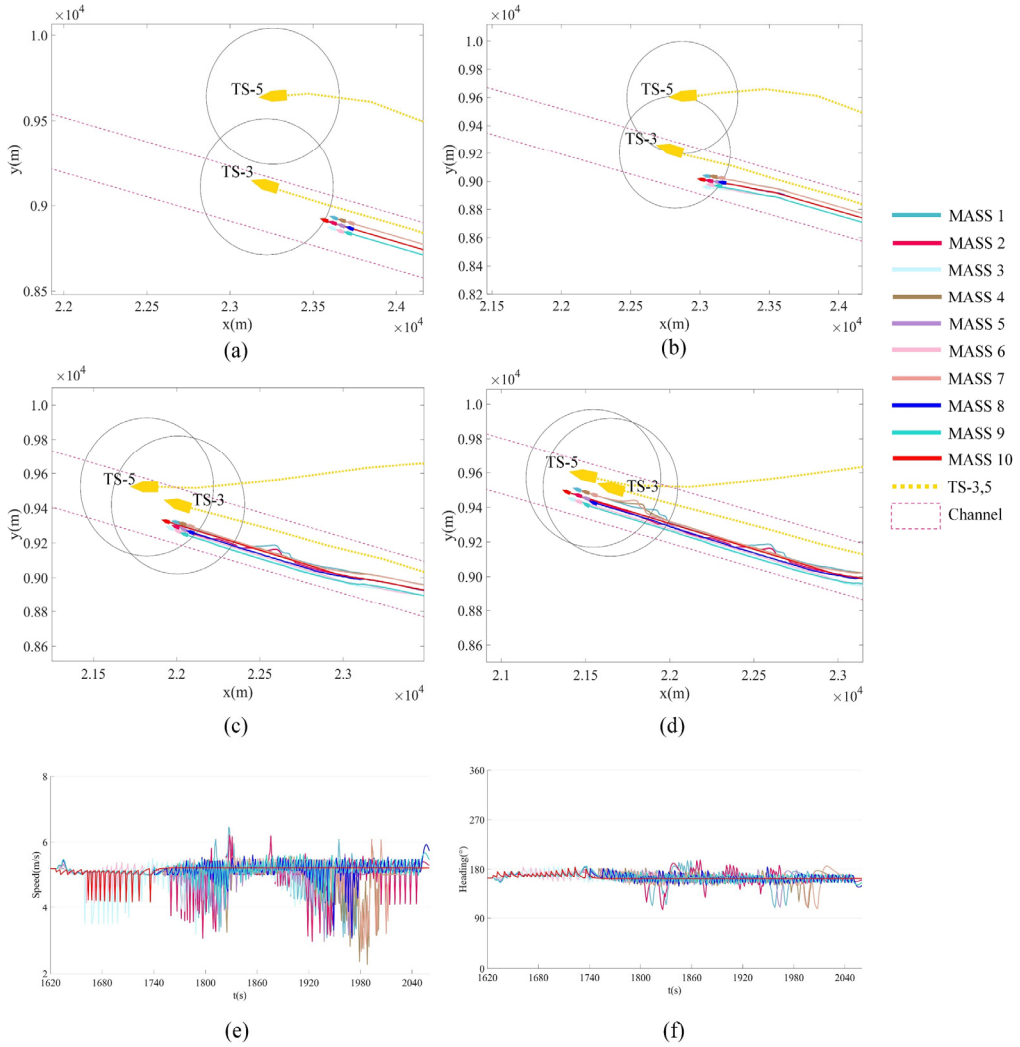

Figure 17. MASS formation encountered two target ship situations. (**a**) About to form an encounter situation with TS-3. (**b**) Gave priority to TS-3 avoidance. (**c**) Avoidance completion of encounter situation with TS-3 and encountered TS-5. (**d**) Avoidance completion of encounter situations to adjust formation pattern. (**e**) MASS speed changes during the situation. (**f**) MASS heading changes during the situation.

5. Conclusions

To resolve the MASS (unmanned ship) formation collision-avoidance and path-following problems, this study improved the APF method and proposed a Formation Ship State Parameter(FSSP). In this article, ENC and AIS data were used to construct a complex navigation environment. The fixed and variable Leader–Follower strategy was adopted and used in the simulation experiment. The Formation Ship State Parameter was defined to check the condition of the F-MASSs during the navigation process, and the priority of the condition determined the MASS action in the next iteration. The F-MASSs encounter with common ships was created by AIS data to verify the designed collision-avoidance regulations of the 'unmanned–manned' encounter situation. The study is limited by the

static environment model without considering the potential influence of wind, waves, and currents, and the MASS kinetic model input is the potential energy without considering the operating characteristics of the ships. The simulation results indicate that the F-MASSs can satisfy the integrated operation of collision avoidance and path following in the constrained environment, and it can support the application of the F-MASS autonomous navigation in the constrained environment, such as port, channel, or island areas. Next, the kinetic model of MASS was considered in the experiment, and the real MASS model was used in the test. In the future, the F-MASS multipath navigation combined with real-time environmental perception will be considered in the process of path following to further improve the intelligence level of MASSs and satisfy automatic collision and risk avoidance.

Author Contributions: Conceptualization, methodology, and writing—original draft preparation, X.C.; conceptualization, methodology, data curation, funding acquisition, and writing—review and editing, M.G.; methodology, investigation, supervision, and project administration, A.Z.; investigation and resources, J.Z.; formal analysis, S.C.; investigation, Z.K.; investigation and resources, H.S.; writing—review and editing, Z.L. All authors have read and agreed to the published version of the manuscript.

Funding: This research is supported by Guangdong Special Fund for Promoting Economic Development (Guangdong Natural Resources Cooperation) (Grant No. [2022]19), the National Natural Science Foundation of China (52201414), Tianjin Research Innovation Project for Postgraduate Students (No. 2021YJSB177), and the Special Fund for Basic Scientific Research Business Expenses of Central Public Welfare Scientific Research Institutes under Grants TKS190302 and TKS20210103.

Institutional Review Board Statement: This study did not require ethical approval.

Informed Consent Statement: Not applicable.

Data Availability Statement: Not applicable.

Conflicts of Interest: The authors declare no conflict of interest.

References

1. IMO Seminar on Development of a Regulatory Framework for Maritime Autonomous Surface Ships (MASS). Available online: https://www.imo.org/en/OurWork/Safety/Pages/MASS.aspx (accessed on 30 October 2022).
2. Annual Overview of Marine Casualties and Incidents 2021. Available online: https://emsa.europa.eu/csn-menu/items.html?cid=14&id=4266 (accessed on 30 October 2022).
3. Kaptan, M.; Uğurlu, Ö.; Wang, J. The effect of nonconformities encountered in the use of technology on the occurrence of collision, contact and grounding accidents. *Reliab. Eng. Syst. Saf.* **2021**, *215*, 107886. [CrossRef]
4. Ntakolia, C.; Lyridis, D.V. A Swarm Intelligence Graph-Based Pathfinding Algorithm Based on Fuzzy Logic (SIGPAF): A Case Study on Unmanned Surface Vehicle Multi-Objective Path Planning. *J. Mar. Sci. Eng.* **2021**, *9*, 1243. [CrossRef]
5. Ma, Y.; Zhao, Y.; Incecik, A.; Yan, X.; Wang, Y.; Li, Z. A collision avoidance approach via negotiation protocol for a swarm of USVs. *Ocean Eng.* **2021**, *224*, 108713. [CrossRef]
6. Qin, Z.; Lin, Z.; Yang, D.; Li, P. A task-based hierarchical control strategy for autonomous motion of an unmanned surface vehicle swarm. *Appl. Ocean Res.* **2017**, *65*, 251–261. [CrossRef]
7. Tong, X.; Zhang, H.; Guo, H. Multi-directional path planning algorithm for unmanned surface vehicle. *J. Comput. Appl.* **2020**, *40*, 3373–3378.
8. Guo, X.; Ji, M.; Zhao, Z.; Wen, D.; Zhang, W. Global path planning and multi-objective path control for unmanned surface vehicle based on modified particle swarm optimization (PSO) algorithm. *Ocean Eng.* **2020**, *216*, 107693. [CrossRef]
9. Lyridis, D.V. An improved ant colony optimization algorithm for unmanned surface vehicle local path planning with multi-modality constraints. *Ocean Eng.* **2021**, *241*, 109890. [CrossRef]
10. Liu, Y.; Bucknall, R. Path planning algorithm for unmanned surface vehicle formations in a practical maritime environment. *Ocean Eng.* **2015**, *97*, 126–144. [CrossRef]
11. Xia, G.; Sun, X.; Xia, X. Multiple Task Assignment and Path Planning of a Multiple Unmanned Surface Vehicles System Based on Improved Self-Organizing Mapping and Improved Genetic Algorithm. *J. Mar. Sci. Eng.* **2021**, *9*, 556. [CrossRef]
12. Zhang, X.; Wang, C.; Jiang, L.; An, L.; Yang, R. Collision-avoidance navigation systems for Maritime Autonomous Surface Ships: A state of the art survey. *Ocean Eng.* **2021**, *235*, 109380. [CrossRef]
13. Wang, N.; Xu, H. Dynamics-Constrained Global-Local Hybrid Path Planning of an Autonomous Surface Vehicle. *IEEE Trans. Veh. Technol.* **2020**, *69*, 6928–6942. [CrossRef]

14. Ning, J.; Chen, H.; Li, T.; Li, W.; Li, C. COLREGs-Compliant Unmanned Surface Vehicles Collision Avoidance Based on Multi-Objective Genetic Algorithm. *IEEE Access* **2020**, *8*, 190367–190377. [CrossRef]
15. Li, Y.; Zheng, J. Real-time collision avoidance planning for unmanned surface vessels based on field theory. *ISA Trans.* **2020**, *106*, 233–242. [CrossRef] [PubMed]
16. Song, A.L.; Su, B.Y.; Dong, C.Z.; Shen, D.W.; Xiang, E.Z.; Mao, F.P. A two-level dynamic obstacle avoidance algorithm for unmanned surface vehicles. *Ocean Eng.* **2018**, *170*, 351–360. [CrossRef]
17. Ni, S.; Liu, Z.; Huang, D.; Cai, Y.; Wang, X.; Gao, S. An application-orientated anti-collision path planning algorithm for unmanned surface vehicles. *Ocean Eng.* **2021**, *235*, 109298. [CrossRef]
18. Liang, X.; Qu, X.; Wang, N.; Li, Y.; Zhang, R. Swarm control with collision avoidance for multiple underactuated surface vehicles. *Ocean Eng.* **2019**, *191*, 106516. [CrossRef]
19. Qi, X.; Cai, Z. Three-dimensional formation control based on nonlinear small gain method for multiple underactuated underwater vehicles. *Ocean Eng.* **2018**, *151*, 105–114. [CrossRef]
20. Kuppan Chetty, R.M.; Singaperumal, M.; Nagarajan, T. Behavior Based Multi Robot Formations with Active Obstacle Avoidance Based on Switching Control Strategy. *Adv. Mater. Res.* **2012**, *433–440*, 6630–6635. [CrossRef]
21. Sun, X.; Wang, G.; Fan, Y.; Mu, D.; Qiu, B. A Formation Autonomous Navigation System for Unmanned Surface Vehicles With Distributed Control Strategy. *IEEE Trans. Intell. Transp. Syst.* **2021**, *22*, 2834–2845. [CrossRef]
22. He, S.; Wang, M.; Dai, S.; Luo, F. Leader–Follower Formation Control of USVs With Prescribed Performance and Collision Avoidance. *IEEE Trans. Ind. Inform.* **2019**, *15*, 572–581. [CrossRef]
23. Zhao, Y.; Ma, Y.; Hu, S. USV Formation and Path-Following Control via Deep Reinforcement Learning With Random Braking. *IEEE Trans. Neural Netw. Learn. Syst.* **2021**, *32*, 5468–5478. [CrossRef] [PubMed]
24. Tonoğlu, F.; Atalar, F.; Başkan, İ.B.; Yildiz, S.; Uğurlu, Ö.; Wang, J. A new hybrid approach for determining sector-specific risk factors in Turkish Straits: Fuzzy AHP-PRAT technique. *Ocean Eng.* **2022**, *253*, 111280. [CrossRef]
25. Christensen, M.; Georgati, M.; Arsanjani, J.J. A risk-based approach for determining the future potential of commercial shipping in the Arctic. *J. Mar. Sci. Technol.* **2022**, *21*, 82–99. [CrossRef]
26. Xiao, F.; Ma, Y. Artificial forces for virtual autonomous ships with encountering situations in restricted waters. *Marit. Policy Manag.* **2020**, *47*, 687–702. [CrossRef]
27. Wang, H.; Liu, J.; Liu, K.; Zhang, J.; Wang, Z. Sensitivity analysis of traffic efficiency in restricted channel influenced by the variance of ship speed. *Proc. Inst. Mech. Eng. M J. Eng.* **2018**, *232*, 212–224. [CrossRef]
28. Xu, X.; Lu, Y.; Liu, X.; Zhang, W. Intelligent collision avoidance algorithms for USVs via deep reinforcement learning under COLREGs. *Ocean Eng.* **2020**, *217*, 107704. [CrossRef]
29. Zhao, Y.; Li, W.; Shi, P. A real-time collision avoidance learning system for Unmanned Surface Vessels. *Neurocomputing* **2016**, *182*, 255–266. [CrossRef]
30. Lyu, H.; Yin, Y. COLREGS-Constrained Real-time Path Planning for Autonomous Ships Using Modified Artificial Potential Fields. *J. Navig.* **2019**, *72*, 588–608. [CrossRef]
31. Wang, S.; Zhang, Y.; Zheng, Y. Multi-ship encounter situation adaptive understanding by individual navigation intention inference. *Ocean Eng.* **2021**, *237*, 109612. [CrossRef]
32. Deng, F.; Jin, L.; Hou, X.; Wang, L.; Li, B.; Yang, H. COLREGs: Compliant Dynamic Obstacle Avoidance of USVs Based on theDynamic Navigation Ship Domain. *J. Mar. Sci. Eng.* **2021**, *9*, 837. [CrossRef]
33. Gao, M.; Shi, G.; Liu, J. Ship encounter azimuth map division based on automatic identification system data and support vector classification. *Ocean Eng.* **2020**, *213*, 107636. [CrossRef]
34. Gao, M.; Kang, Z.; Zhang, A.; Liu, J.; Zhao, F. MASS autonomous navigation system based on AIS big data with dueling deep Q networks prioritized replay reinforcement learning. *Ocean Eng.* **2022**, *249*, 110834. [CrossRef]